

## RESEARCH ARTICLE OPEN ACCESS

# Microstructure-dependent abrasive wear behavior of metallic alloys under tumbling abrasion

## Mikrostrukturabhängiges abrasives Verschleißverhalten metallischer Legierungen unter Trommelabrieb

R. L. P. Teixeira<sup>1</sup>  | S. O. Cardoso<sup>1</sup> | J. C. de Lacerda<sup>1</sup> | R. N. Penha<sup>1</sup>  | R. F. Brito<sup>1</sup> | T. G. de Brito<sup>1</sup> | V. G. de Moraes<sup>1</sup> | A. B. Henriques<sup>2</sup>

<sup>1</sup>Federal University of Itajubá, Campus Prof. José Rodrigues Seabra, Av. B P S, 1303 - Pinheirinho, Itajubá, MG 37500-903, Brazil | <sup>2</sup>Federal University of Minas Gerais, Department of Metallurgical and Materials Engineering, Av. Antônio Carlos 6627, Pampulha, Belo Horizonte, MG 31270-901, Brazil

**Correspondence:** R. L. P. Teixeira ([ricardo.luiz@unifei.edu.br](mailto:ricardo.luiz@unifei.edu.br))

**Received:** 3 July 2025 | **Revised:** 17 September 2025 | **Accepted:** 11 February 2026

**Keywords:** abrasion mechanisms | wear resistance | carbide morphology | ferrous alloys | tumbling test

**Schlüsselwörter:** Abriebmechanismen | Verschleißbeständigkeit | Karbidmorphologie | Eisenlegierungen | Trommelverschleißprüfung

### ABSTRACT

Grinding media consumption accounts for a significant portion of total operational expenses in mineral processing, reaching up to 45 %. This study examines the correlation between microstructure and abrasive wear resistance of metallic alloys under tumbling abrasion, with a focus on practical applications in mineral processing. The novelty lies in establishing systematic links between carbide morphology, matrix hardness, and wear mechanisms in environments of quartz sand and iron ore. Abrasive wear tests were conducted using the SSAB (Swedish Steel AB) tumbling abrasion method, which represents high-stress wet grinding conditions involving ball–ball and ball–drum collisions, as also defined in previous laboratory ball mill investigations and in more recent analyses of abrasion classification in grinding media. The results show that high-chromium cast irons exhibit the lowest wear rates (0.18 cm<sup>3</sup>/week), while low-alloy steels experience up to five times greater volumetric loss (0.91 cm<sup>3</sup>/week). Scanning electron microscopy reveals micro-grooving and matrix detachment in more complex alloys, whereas softer steels display significant corrosion-assisted pitting and cracking. These findings provide practical guidelines for alloy design and the selection of grinding media, underscoring the importance of microstructural control in tailoring materials to specific abrasive environments.

### ZUSAMMENFASSUNG

Der Verbrauch von Mahlkörpern macht einen erheblichen Anteil der gesamten Betriebskosten in der Aufbereitungstechnik aus und kann bis zu 45 % erreichen. Diese Arbeit untersucht den Zusammenhang zwischen Mikrostruktur und Abrasivverschleißbeständigkeit metallischer Legierungen unter Trommelabrieb, mit besonderem Fokus auf praktische Anwendungen in der Erzaufbereitung. Die Neuheit liegt in der systematischen Verknüpfung von Karbidmorphologie, Matrixhärte und Verschleißmechanismen in Umgebungen mit Quarzsand und Eisenerz. Die Abrasivverschleißprüfungen

This is an open access article under the terms of the [Creative Commons Attribution](https://creativecommons.org/licenses/by/4.0/) License, which permits use, distribution and reproduction in any medium, provided the original work is properly cited.

© 2026 The Author(s). *Materialwissenschaft und Werkstofftechnik* published by Wiley-VCH GmbH.

wurden nach der SSAB-Trommelabriebmethode (Swedish Steel AB) durchgeführt, die Hochlast-Nassmahlbedingungen mit Kugel-Kugel- und Kugel-Trommel-Kollisionen abbildet, wie sie auch in früheren Labor-Kugelmühlenuntersuchungen sowie in neueren Analysen zur Klassifizierung des Abriebs bei Mahlkörpern beschrieben wurden. Die Ergebnisse zeigen, dass hochchromhaltige Gusseisen (high-chromium cast iron) die geringsten Verschleißraten aufweisen ( $0,18 \text{ cm}^3/\text{Woche}$ ), während niedriglegierte Stähle einen bis zu fünffach höheren Volumenverlust erleiden ( $0,91 \text{ cm}^3/\text{Woche}$ ). Rasterelektronenmikroskopische Untersuchungen (REM/SEM) zeigen Mikroriefenbildung und Matrixablösung in komplexeren Legierungen, wohingegen weichere Stähle deutliche korrosionsunterstützte Lochfraßbildung (Pitting) und Rissinitiierung aufweisen. Diese Ergebnisse liefern praxisorientierte Leitlinien für die Legierungsentwicklung und die Auswahl geeigneter Mahlkörpermaterialien und unterstreichen die Bedeutung der Mikrostrukturkontrolle bei der Anpassung von Werkstoffen an spezifische Abrasivumgebungen.

## 1 | Introduction

Grinding operations in mineral processing are energy-intensive and contribute significantly to overall operational costs [1-5]. Among these, the consumption of grinding media can represent up to 45 % of the total expenditure [6-9]. Consequently, the selection of wear-resistant materials is crucial to enhancing grinding efficiency and reducing production downtime [10-13].

Common grinding media include low-alloy martensitic steels and high-chromium white cast irons [14-16]. These materials are selected for their balance between hardness, abrasion resistance, and mechanical integrity [17-19]. Despite their widespread use, the relationship between microstructure and wear performance across various abrasive conditions has been studied extensively over the past decades; however, systematic comparative data across different abrasives (e. g., quartz sand vs. iron ore) remain limited [20-26]. This study contributes incremental insights by reinforcing established principles with controlled laboratory testing of commercial alloys.

This study aims to address this gap by investigating eight commercially available metallic alloys—two high-chromium white cast irons and six low-alloy steels—under controlled laboratory conditions. The alloys were tested in both quartz sand and iron ore media, and their performance was evaluated based on their microstructural features, hardness profiles, and wear resistance. The goal is to establish correlations that support the development of grinding media tailored to specific abrasive environments in mineral processing.

Grinding media consumption accounts for a significant operational cost in mineral processing, often exceeding 45 % of total expenses. Thus, selecting materials with optimized wear resistance is crucial for enhancing grinding efficiency and reducing costs [2,14,27-29]. Common grinding media include low-alloy martensitic steels and high-chromium white cast irons, typically exhibiting hardness values of 60 HRC-65 HRC [30]. However, balancing hardness for abrasion resistance with ductility to prevent fracture remains a challenge [16].

Although several studies have evaluated the performance of grinding media, few works have systematically correlated microstructural features with abrasive wear under wet grinding conditions. This study addresses this gap by analyzing eight metallic alloys, linking carbide morphology and hardness to wear resistance in industrially relevant conditions [31]. This is especially true under wet grinding conditions that are representative of industrial practice. To address this gap, this study investigates eight commercially relevant metallic alloys, linking their microstructures to wear behavior in quartz sand and iron ore using a laboratory-scale tumbling abrasion test [14,32,33]. The findings

aim to enhance the understanding of material selection for grinding media across diverse operational settings.

## 2 | Materials and methods

Eight commercially available metallic alloys were evaluated, including two high-chromium white cast irons and six low-alloy carbon steels. Each alloy was characterized by chemical composition, microstructure, and hardness. Elemental analysis was performed using Optical Emission Spectrometry (OES), following standard metallurgical procedures [34]. Microstructures were examined via optical microscopy after conventional metallographic preparation, which involved grinding, polishing, and etching with a nital solution [2].

Hardness measurements were conducted using the Rockwell C scale (HRC), which provides both surface and core values to assess hardness gradients induced by heat treatment [35-38]. Heat treatments were applied before testing: steels (C-H) were austenitised at  $850 \text{ }^\circ\text{C}$ – $900 \text{ }^\circ\text{C}$  for 1 h, quenched in oil, and tempered at  $200 \text{ }^\circ\text{C}$  for 2 h; white cast irons (A-B) were austenitised at  $950 \text{ }^\circ\text{C}$  for 2 h, air-cooled, and tempered at  $300 \text{ }^\circ\text{C}$  for 2 h. The abrasive wear resistance of the alloys was assessed using the SSAB tumbling abrasion method, essentially a small laboratory ball mill (800 mm internal diameter  $\times$  300 mm length,  $45 \text{ min}^{-1}$ ), initially developed by Swedish Steel AB. This apparatus simulates the high-stress wet abrasion conditions of industrial grinding, where wear arises from ball-ball and ball-drum collisions in abrasive slurry [27].

Wear tests were conducted in a horizontal, cylindrical steel drum (800 mm internal diameter, 300 mm in length) that rotated at  $45 \text{ min}^{-1}$ . The drum was partially filled with 3000 g of abrasive material, specifically quartz sand (AFS 30/40) and iron ore collected from an industrial grinding circuit, and 1000 mL of water to simulate low-stress wet grinding conditions. Four specimens of each alloy were machined into spherical shapes, each with a diameter of  $25 \text{ mm} \pm 0.1 \text{ mm}$ , to replicate industrial grinding media. All 32 specimens were tested simultaneously in the drum mill, where wear was dominated by high-stress abrasion caused by ball-ball and ball-drum impacts in abrasive slurry. Steels (C-H) were prepared from hot-rolled bar stock, and high-chromium cast irons (A-B) from cast blocks. All specimens were machined to this geometry to ensure identical size and surface finish before testing. After one week of tumbling, specimen mass loss was measured using a precision digital balance, and volumetric loss was calculated from density values obtained by metallographic analysis. Scanning electron microscopy (SEM) was employed to

characterize the wear mechanisms, with parameters specified for accelerating voltage, working distance, and magnification. The selection of these conditions was based on their relevance to reproducing industrial environments and ensuring accurate assessment of microstructural effects on wear resistance [33,39].

Each alloy was characterized by chemical composition using optical emission spectrometry (OES), microstructural analysis via optical microscopy, and surface and core hardness using the Rockwell C scale. Scanning electron microscopy analysis was employed to examine the worn surface features, including grooves, pitting, and cracking. To interpret the wear performance, the Archard wear model was applied, where volumetric loss ( $V$ ) is related to load ( $L$ ), sliding distance ( $d$ ), and hardness ( $H$ ) through a wear coefficient ( $k$ ), expressed as  $V = k \times (L \times d)/H$ .

$$V = k \times (L \times d)/H \quad (1)$$

This model provided a theoretical framework for evaluating the abrasion resistance of each alloy under consistent test conditions.

To further investigate the wear mechanisms involved, selected specimens are examined using scanning electron microscopy (SEM). Scanning electron microscopy analysis enabled the identification of characteristic wear features, including abrasive grooves, microcracks, pitting, and corrosion-induced damage. These surface observations are correlated with the alloy compositions and microstructures for a better understanding of the interaction between the abrasive environment and material response [28]. The SSAB tumbling test methodology proved to be a reliable and representative approach for evaluating the wear resistance of grinding media materials under realistic service conditions in the mineral processing industry [27].

The wear behavior was further interpreted using the Archard wear model, Equation (1), which relates the volumetric loss ( $V$ ) to the applied load ( $L$ ), the sliding distance ( $d$ ), and the material hardness ( $H$ ) through the wear coefficient.

This model assumes a linear relationship between wear and load-distance products, inversely proportional to hardness. Although simplified, the Archard equation provides a sound theoretical framework for evaluating the abrasion resistance

of different metallic alloys under similar loading and environmental conditions.

### 3 | Results and discussion

The results demonstrate significant differences in abrasive wear behavior among the evaluated alloys when exposed to quartz sand and iron ore media. Quartz sand, due to its higher angularity and hardness, produced greater volumetric loss across all samples compared to iron ore. Figure 1 presents the weekly volume loss for all tested materials. High-chromium white cast irons (samples A and B) exhibited the lowest wear, while cast carbon steel (sample C) showed the highest loss, particularly in the quartz sand environment.

Figures 1(A) and 1(B) show the weekly volume loss for all materials in sand and iron ore media, respectively. The results indicate that quartz sand caused higher volumetric wear compared to iron ore for most grinding media (samples). This trend can be explained by the higher hardness and angularity of the quartz sand particles, which promote more intense cutting and gouging actions on the sample surfaces.

Volumetric wear loss is calculated from the measured mass loss and the density of each alloy. Figures 2(A) and 2(B) compare the final cumulative volumetric losses after one week of testing materials in (a) sand and (b) iron ore media. High-chromium white cast irons (samples A and B) exhibited the lowest wear rates in both media. In contrast, the cast carbon steel (sample C) shows the highest volumetric loss, especially in the quartz sand environment. Forged low-alloy carbon steels (samples D to H) demonstrate intermediate wear resistance, with consistent performance across both abrasive types.

Wear behavior shows greater variability in quartz sand. This is reflected in the standard deviation of mass loss shown in Figure 3A, B. This variability is linked to localized surface interactions between the hard quartz grains and microstructural heterogeneities in the alloys.

These results emphasize the importance of matching grinding media composition to the specific abrasive environment. The

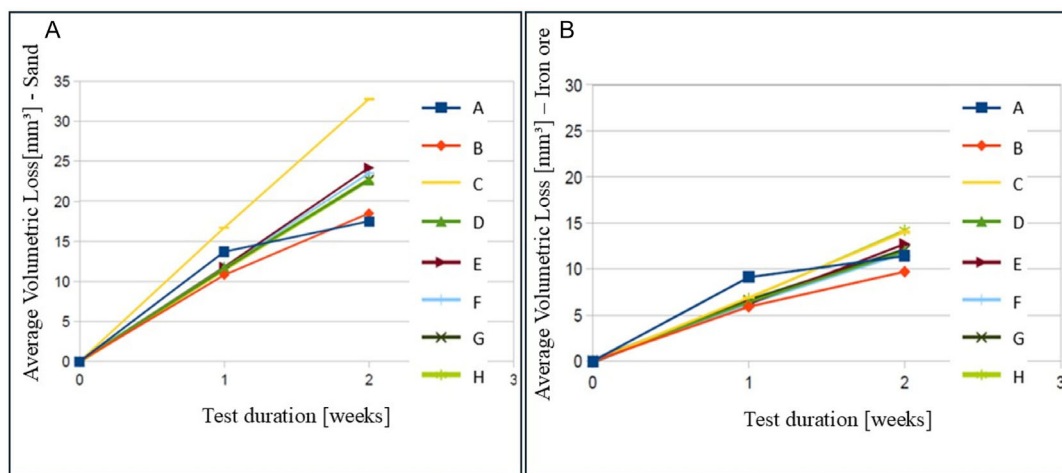


**FIGURE 1** | Weekly volumetric loss ( $\text{cm}^3/\text{week}$ ) of metallic grinding media tested under tumbling abrasion in (A) quartz sand and (B) iron ore environments. Results indicate that the relative wear severity induced by abrasive type varies, with quartz sand producing higher material loss due to its angularity and hardness.

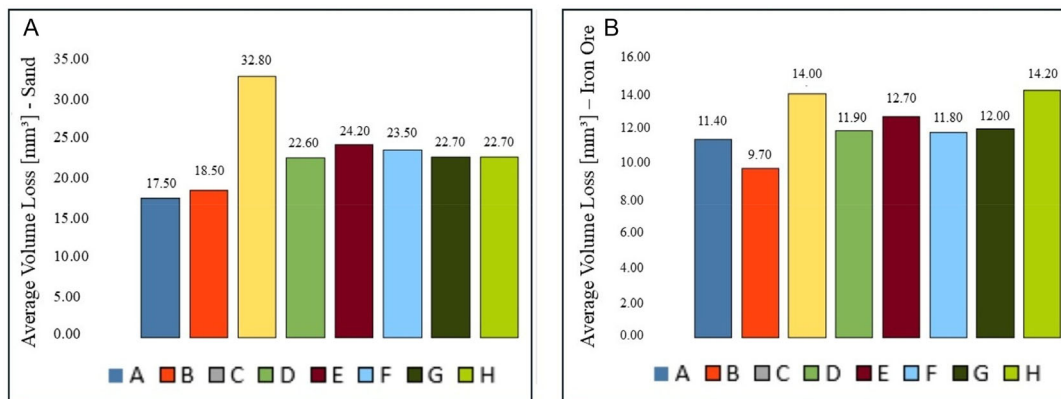


**FIGURE 2** | Cumulative average volumetric wear loss ( $\text{cm}^3$ ) of eight metallic alloys after one week of tumbling abrasion in (A) quartz sand and (B) iron ore. The values are derived from mass loss measurements and material densities, reflecting total degradation under test conditions.

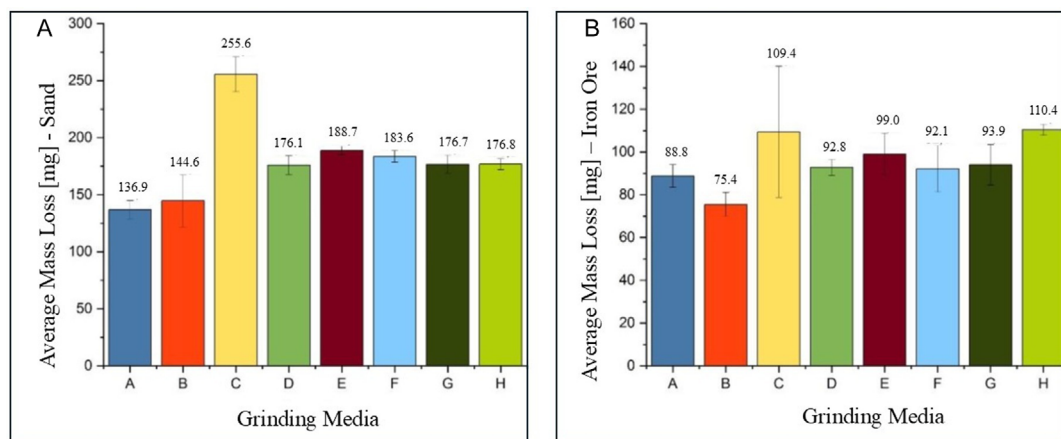


**FIGURE 3** | Standard deviation of mass loss (g) for grinding media samples tested in (A) quartz sand and (B) iron ore. The variation highlights the influence of abrasive particle interaction and microstructural heterogeneity on the repeatability of wear.

superior performance of high-chromium cast irons suggests that their complex carbide-rich microstructure contributes significantly to wear resistance in both abrasive regimes.

The current research highlights the advantageous properties of high-chromium cast irons in abrasive environments characterized by harsh quartz sand. The robust carbide structure inherent in these materials demonstrates superior performance relative to low-alloy steels, which may only be suitable for the milder conditions associated with iron ore abrasion. This evidence serves as a critical reference for selecting strategic materials within mineral processing plants. Such choices can significantly influence both operational efficiency and long-term durability, thereby offering valuable guidance for engineers and decision-makers in the field. This offers practical advice on material selection in mineral processing plants.

### 3.1 | Microstructure–performance relationship

Table 1 presents the chemical composition of the eight alloys analyzed, which was determined using OES with spark excitation, a technique commonly employed for multi-elemental analysis of ferrous alloys. The materials are organized into two main categories: high-chromium white cast irons (samples A and B,

with approximately 12.9 wt.-% Cr) and low-alloy carbon steels (samples C-D, with up to 2.5 wt.-% alloying elements). The carbon content ranged from 0.85 wt.-% to 3.2 wt.-%, with higher values found in the cast irons, Table 1.

Optical microscopy reveals that the high-chromium cast irons contained a martensitic matrix reinforced by eutectic carbides, mainly  $(\text{Fe,Cr})_7\text{C}_3$  and Fe-rich  $(\text{Fe,Cr})_3\text{C}$ . The steels exhibit martensitic microstructures, often with small fractions of pearlite and retained austenite. These differences directly influenced hardness and, consequently, wear resistance.

The chemical composition of cast irons controls the type of carbides formed [29]. High-chromium cast irons, with around 12.9 wt.-% Cr, tends to form  $\text{M}_7\text{C}_3$  carbides [40,41]. These carbides are hard and improve wear resistance. In cast irons with lower chromium content,  $\text{M}_3\text{C}$  (cementite,  $\text{Fe}_3\text{C}$ ) is the predominant carbide, with only minor fractions of  $\text{M}_7\text{C}_3$  possibly promoted by silicon.

In contrast, higher chromium levels favor the formation of  $\text{M}_{23}\text{C}_6$  carbides [42,43]. Carbide formation depends on the levels of carbon and alloying elements, mainly chromium. Solidification and heat treatment also affect the type and distribution of carbides. As a result, the alloy composition has a direct impact on wear performance.

**TABLE 1** | Chemical composition (wt.-%) of metallic alloys used as grinding media in tumbling abrasion tests. Samples A and B are high-chromium white cast irons, while samples C to H are low-alloy carbon steels. Elements were quantified using optical emission spectrometry (OES) and grouped by metallurgical classification to highlight the alloy design strategies that affect wear behavior.

Grinding Media [samples]	C [wt.-%]	Si [wt.-%]	Mn [wt.-%]	Cr [wt.-%]	Mo [wt.-%]	Ni [wt.-%]
A	3.20	1.26	1.05	12.90	1.97	0.96
B	3.21	1.25	1.01	7.60	1.88	0.95
C	0.92	0.20	0.94	0.65	0.04	0.01
D	0.85	0.22	0.95	0.68	0.05	0.01
E	0.88	0.21	0.96	0.70	0.06	0.01
F	0.90	0.23	0.97	0.72	0.07	0.01
G	0.93	0.22	0.96	0.69	0.06	0.01
H	0.91	0.23	0.96	0.65	0.03	0.01

**TABLE 2** | Surface and core hardness values (Rockwell C, HRC) for metallic grinding media samples A to H. Hardness was measured using the Rockwell C scale at both surface and core regions to assess through-thickness hardness gradients resulting from heat treatment. Results are reported as mean  $\pm$  standard deviation for four specimens per alloy.

Grinding media [samples]	Surface hardness (Mean $\pm$ SD) [HRC]	Core hardness (mean $\pm$ SD) [HRC]
A	68.2 $\pm$ 0.5	59.0 $\pm$ 0.6
B	67.5 $\pm$ 0.4	58.2 $\pm$ 0.5
C	62.3 $\pm$ 0.8	53.5 $\pm$ 0.9
D	65.1 $\pm$ 0.6	55.8 $\pm$ 0.7
E	66.7 $\pm$ 0.5	57.4 $\pm$ 0.6
F	64.8 $\pm$ 0.6	56.2 $\pm$ 0.5
G	66.0 $\pm$ 0.7	55.9 $\pm$ 0.6
H	67.2 $\pm$ 0.5	57.1 $\pm$ 0.7

Table 2 presents the estimated Rockwell C hardness (HRC) values for eight different metallic alloys, labeled A through H. The hardness measurements range from 53 HRC to 69 HRC. The values include the mean and standard deviation for both surface and core regions. The low-alloy steels exhibit surface hardness values higher than those at the core, indicating a hardness gradient consistent with through-hardening, where the surface is slightly harder than the core, as expected in heat-treated grinding media [36-38,44]. Alloys A and B show the highest surface hardness, with values close to 68 HRC, while alloy C presents the lowest core hardness, around 53.5 HRC. The harder phases in the cast irons, particularly the carbides, are responsible for deflecting or resisting abrasive action, leading to reduced material loss during testing. In all samples, the surface hardness is consistently higher than the core hardness. The low standard deviations suggest uniform heat treatment and reliable measurements. These hardness values contribute to understanding the wear resistance behavior of each alloy.

The performance index, derived from normalized volumetric losses, provides an alternative representation of the same wear

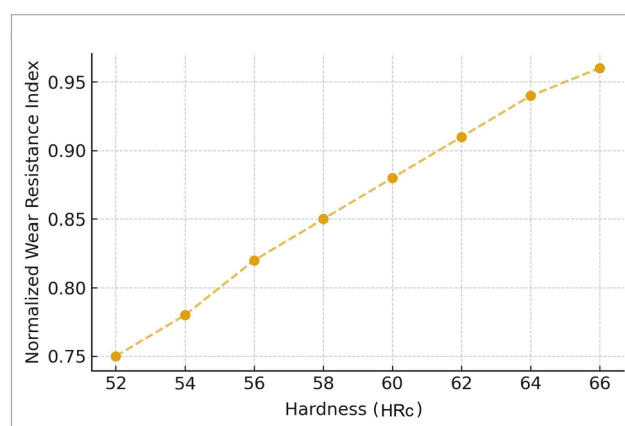


**FIGURE 4** | Relationship between normalized wear resistance index and hardness (HRC) for metallic grinding media tested in: (a) quartz sand and (b) iron ore. Higher hardness generally correlates with superior wear resistance.

data, highlighting the superior relative behavior of the cast irons. Figure 4 further illustrates this relationship by plotting the normalized wear resistance index directly against the measured hardness values, which evidences a positive correlation between hardness and wear resistance. Figure 5A, B present the relative performance of all samples in sand and iron ore environments, respectively.

The linear trend in volumetric loss for most materials in quartz sand indicates a constant wear rate, while in iron ore, the wear rates are lower and less variable. These findings align with previous observations regarding the milder abrasive nature of iron ore [45,46].

### 3.2 | Scanning electron microscopy surface analysis

Post-test scanning electron microscopy analysis provides insights into the wear mechanisms acting on the samples. Figure 6 shows representative micrographs of the worn surfaces for samples A to D, while Figure 7 displays the same for samples E to H.

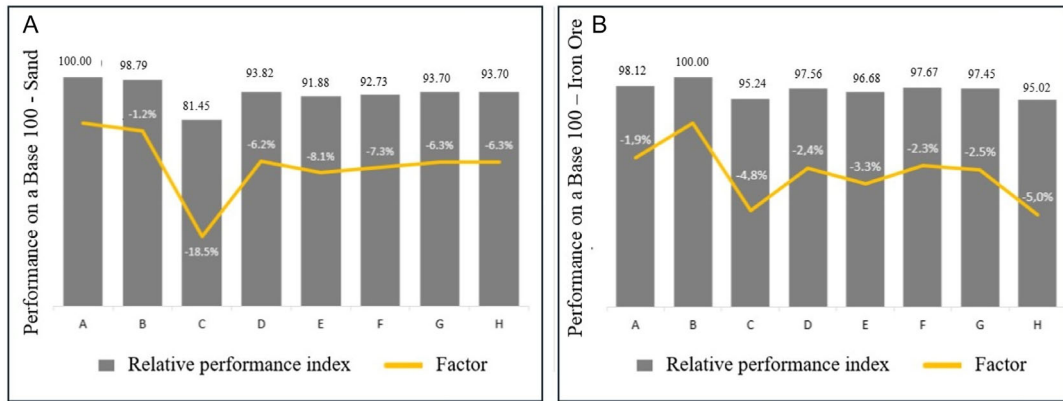


**FIGURE 5** | Normalized wear resistance index of metallic grinding media based on volumetric loss data in (A) quartz sand and (B) iron ore environments. Higher values indicate superior abrasion resistance. This metric enables the comparative assessment of performance across different abrasive regimes.

In the high-chromium cast irons, selective matrix wear is observed between carbide phases, with evidence of micro-grooving and limited matrix detachment of the metallic matrix. This behavior is consistent with the role of hard carbides, which act as barriers to abrasive penetration, thereby promoting greater surface integrity and contributing to wear resistance [16,47-52].

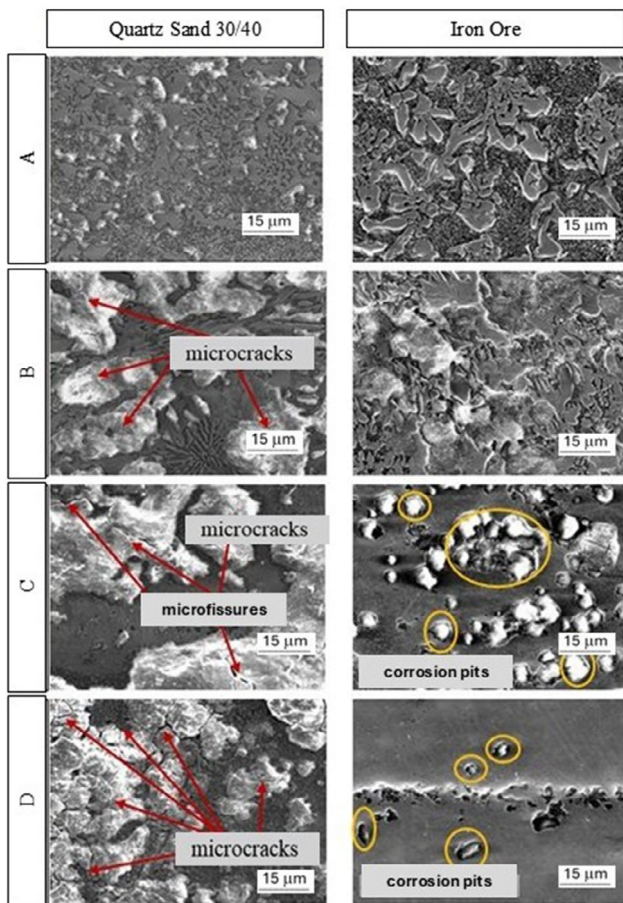


**FIGURE 6** | Scanning electron microscopy micrographs of worn surfaces of samples A to D after tumbling abrasion. Samples A and B (high-chromium white cast irons) show selective matrix wear and micro-grooving between carbide phases. Samples C and D (low-alloy steels) exhibit pronounced corrosion pitting and microcracking, particularly under quartz sand exposure. The performance index.

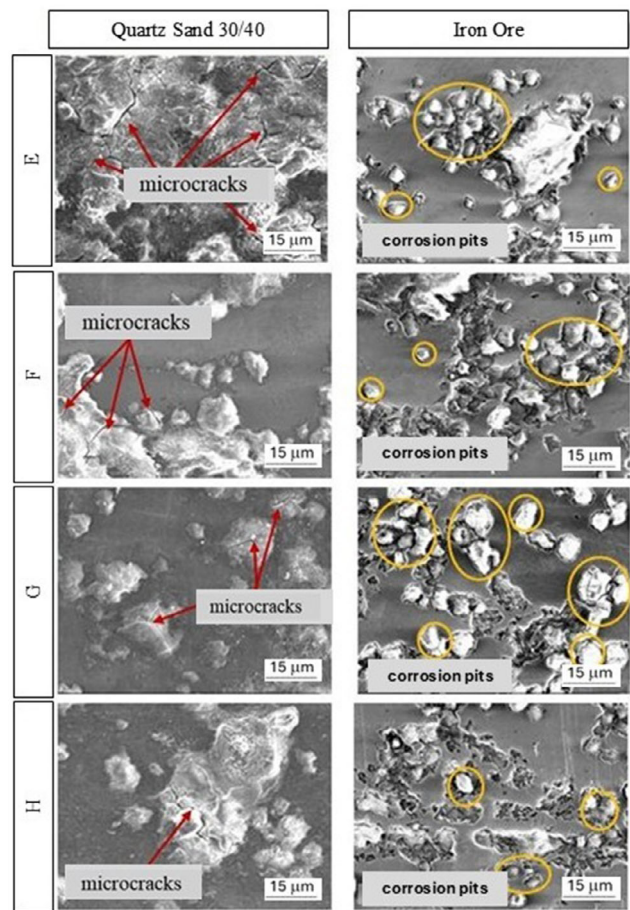


**FIGURE 7** | Scanning electron microscopy images of worn surfaces for samples E to H (low-alloy forged steels) following tumbling abrasion tests. The surfaces reveal characteristic wear features including shallow grooving, localized cracking, and corrosion-assisted pitting, which correlate with microstructural variations and hardness gradients.

In contrast, the low-alloy steel samples exhibited extensive corrosion pitting and microcracking, particularly in the quartz sand environment. The formation of pits suggests a significant contribution from corrosion-assisted wear, which, under the low-stress conditions of the experimental setup, may exceed pure abrasive mechanical wear [2,34,53-58].

These observations underscore the significance of microstructure in influencing the wear performance of materials. The interaction between hard phases and corrosion resistance, particularly in chromium-rich cast irons, is a crucial factor in achieving superior durability in environments subjected to abrasive and corrosive conditions.

#### 4 | Conclusions

This study demonstrated a strong correlation between microstructure and abrasive wear resistance in metallic alloys used as grinding media. High-chromium white cast irons exhibited the highest wear resistance, attributed to their hard martensitic matrices and high-volume fractions of chromium carbides. In contrast, low-alloy carbon steels presented significantly higher volumetric losses, particularly under the more aggressive quartz sand environment.

Distinct wear mechanisms were observed based on alloy composition and abrasive type. Harder alloys predominantly exhibited micro-grooving and abrasion, while corrosion-assisted pitting and cracking were more prevalent in softer steels. Scanning electron microscopy analyses supported these observations.

The variation in alloy performance across abrasive conditions highlights the need for application-specific material selection. The findings offer a scientific basis for optimizing grinding media design through tailored alloying and heat treatment strategies. Such improvements are essential for enhancing durability, reducing media consumption, and improving the operational efficiency of mineral processing systems.

These differences highlight the crucial role of microstructural constituents, such as carbide morphology, volume fraction, and distribution, in determining wear behavior under various abrasive conditions. A detailed scanning electron microscopy analysis of the worn surfaces revealed distinct wear mechanisms, depending on the alloy and abrasive type. Mechanical abrasion was predominant in high-hardness alloys, while corrosion-assisted degradation was especially pronounced in low-alloy steels under aqueous conditions.

Furthermore, the reversal in wear resistance ranking between quartz sand and iron ore abrasives highlighted the substantial impact of operating conditions on grinding media performance. This indicated that materials with superior performance in one abrasive regime may underperform in another, reinforcing the necessity for application-specific material selection.

The findings established a solid foundation for developing more durable, application-optimized, and cost-effective grinding media. Tailoring microstructure via alloying strategies and heat treatments emerged as a promising approach to enhance wear resistance while preserving industrial toughness requirements. These improvements could lead to significant reductions in operational downtime, grinding media consumption, and energy use, contributing to more efficient and sustainable mineral processing operations.

#### Author Contributions

R. L. P. Teixeira: Conceptualization, Methodology, Writing – Original Draft. S. O. Cardoso: Investigation, Data curation, Writing – Original Draft. J. C. de Lacerda, R. N. Penha: Validation, Formal analysis.

R. F. de Brito, T. G. de Brito Filho, V. G. de Moraes, A. B. Henriques: Supervision, Writing – Review & Editing.

#### Acknowledgements

The authors wish to express their heartfelt gratitude to the PRPPG - Postgraduate Program in Materials Engineering at the Federal University of Itajubá, as well as the Institute of Integrated Engineering at the same institution.

The Article Processing Charge for the publication of this research was funded by the Coordenação de Aperfeiçoamento de Pessoal de Nível Superior - Brasil (CAPES) (ROR identifier: 00x0ma614).

#### Financial disclosure

This article was submitted by authors from the Federal University of Itajubá (UNIFEI), a CAPES-affiliated institution eligible under the Wiley Transformative Agreement for APC coverage and Open Access publication.

#### Conflict of interest

The authors declare no financial or commercial conflict of interest.

#### Data availability statement

The data that support the findings of this study are available from the corresponding author upon reasonable request.

#### References

1. T. Igogo, K. Awuah-Offei, A. Newman, T. Lowder, and J. Engel-Cox, "Integrating renewable energy into mining operations: Opportunities, challenges, and enabling approaches," *Applied Energy* 300 (2021): 117375. <https://doi.org/10.1016/j.apenergy.2021.117375>.
2. N. Qian, J. Chen, A. M. Khan, N. He, L. Li, and Y. Xu, "Towards Sustainable Grinding of Difficult-to-Cut Alloys—A Holistic Review and Trends," *Chinese Journal of Mechanical Engineering* 37, no. 1 (2024): 23. <https://doi.org/10.1186/s10033-024-01002-y>.
3. A. Kumar, R. Sahu, and S. K. Tripathy, "Energy-Efficient Advanced Ultrafine Grinding of Particles Using Stirred Mills—A Review," *Energies* 16, no. 14 (2023): 5277. <https://doi.org/10.3390/en16145277>.
4. S. O. Oweh, P. A. Aigba, O. D. Samuel, et al., "Improving Productivity at a Marble Processing Plant Through Energy and Exergy Analysis," *Sustainability* 16, no. 24 (2024): 11233. <https://doi.org/10.3390/su162411233>.
5. Z. X. Zhang, J. A. Sanchidrián, F. Ouchterlony, and P. Moser, "Reduction of Fragment Size from Mining to Mineral Processing: A Review," *Rock Mechanics and Rock Engineering* 56, no. 1 (2023): 747–778. <https://doi.org/10.1007/s00603-022-03068-3>.
6. M. M. Bwalya, O. S. Samukute, and N. Chimwani, "SAG Mill Grinding Media Stress Evaluation—A DEM Approach," *Minerals* 15, no. 4 (2025): 431. <https://doi.org/10.3390/min15040431>.
7. X. Zhang, Y. Han, and S. K. Kawatra, "Effects of Grinding Media on Grinding Products and Flotation Performance of Sulfide Ores," *Mineral Processing and Extractive Metallurgy Review* 42, no. 3 (2021): 172–183. <https://doi.org/10.1080/08827508.2019.1692831>.
8. Q. Lu, Y. Chen, and X. Zhang, "Grinding process optimization considering carbon emissions, cost and time based on an improved dung beetle algorithm," *Computers & Industrial Engineering* 197 (2024): 110600. <https://doi.org/10.1016/j.cie.2024.110600>.
9. K. Kishore, M. K. Sinha, A. Singh, Archana, M. K. Gupta, and M. E. Korkmaz, "A comprehensive review on the grinding process: Advancements, applications and challenges," *Proceedings of the Institution of Mechanical Engineers, Part C: Journal of Mechanical*

- Engineering Science* 236, no. 22 (2022): 10923–10952. <https://doi.org/10.1177/09544062221110782>.
10. W. Zhai, L. Bai, R. Zhou, et al., “Recent Progress on Wear-Resistant Materials: Designs, Properties, and Applications,” *Advanced Science* 8, no. 11 (2021): 2003739. <https://doi.org/10.1002/advs.202003739>.
  11. Y. Wang, D. Li, C. Nie, et al., “Research Progress on the Wear Resistance of Key Components in Agricultural Machinery,” *Materials* 16, no. 24 (2023): 7646. <https://doi.org/10.3390/ma16247646>.
  12. N. Askarxodjayev, J. G. G'ayratov, G. G. Isakov, et al., “Study of Surface Hardening of High-Manganese Steel 110G13L,” *Materials Today: Proceedings* 108 (2024): 32–36. <https://doi.org/10.1063/5.0091543>.
  13. S. Antony Jose, Z. Lapierre, T. Williams, et al., “Wear- and Corrosion-Resistant Coatings for Extreme Environments: Advances, Challenges, and Future Perspectives,” *Coatings* 15, no. 8 (2025): 878. <https://doi.org/10.3390/coatings15080878>.
  14. N. Matsanga, W. Nheta, and N. Chimwani, “A Review of the Grinding Media in Ball Mills for Mineral Processing,” *Minerals* 13, no. 11 (2023): 1373. <https://doi.org/10.3390/min13111373>.
  15. U. Wendt, “Engineering Materials and Their Properties,” in *Springer Handbook of Mechanical Engineering*, ed. K.-H. Grote and H. Hefazi (Cham: Springer International Publishing, 2021), 233–292.
  16. S. Fashu and V. Trabadelo, “Development and Performance of High Chromium White Cast Irons (HCWCIs) for Wear-Corrosive Environments: A Critical Review,” *Metals* 13, no. 11 (2023): 1831. <https://doi.org/10.3390/met13111831>.
  17. Y. Huang, G. Liu, G. J. Xiao, and J. Y. Xu, “Abrasive belt grinding force and its influence on surface integrity,” *Materials and Manufacturing Processes* 38, no. 7 (2023): 888–897. <https://doi.org/10.1080/10426914.2022.2116042>.
  18. Y. Cheng, Y. Wang, J. Lin, et al., “Research status of the influence of machining processes and surface modification technology on the surface integrity of bearing steel materials,” *The International Journal of Advanced Manufacturing Technology* 125, no. 7-8 (2023): 2897–2923. <https://doi.org/10.1007/s00170-023-10960-x>.
  19. M. J. Jackson and M. J. Toward, “Grinding and Abrasive Machining of Composite Materials,” in *Advances in Machining of Composite Materials*, ed. I. Shyha and D. Huo (Cham: Springer International Publishing, 2021), 459–483.
  20. W. Ding, B. Zhao, Q. Zhang, and Y. Fu, “Fabrication and wear characteristics of open-porous cBN abrasive wheels in grinding of Ti–6Al–4V alloys,” *Wear* 477 (2021): 203786. <https://doi.org/10.1016/j.wear.2021.203786>.
  21. W. Liu, T. Jiang, S. Wei, et al., “A comparative analysis of abrasive wear behaviors and mechanisms of pearlitic and carbide-free bainitic steels for grinding mill liners under varied impact loads,” *Wear* 566–567 (2025): 205765. <https://doi.org/10.1016/j.wear.2025.205765>.
  22. S. Liu, M. Liu, T. Liu, H. Xiao, and B. Xiao, “Wear characteristics of brazing diamond abrasive wheel on high efficiency grinding ferrous metals,” *Wear* 514–515 (2023): 204580. <https://doi.org/10.1016/j.wear.2022.204580>.
  23. P. Hosseini, N. Gharib, J. F. Derakhshandeh, and P. Radziszewski, “Exploring an Energy-Based Model in Comminution,” *Journal of Tribology* 144, no. 4 (2022): 041201. <https://doi.org/10.1115/1.4052780>.
  24. B. A. Miller, R. J. Shipley, R. J. Parrington, et al., “Abrasive Wear Failures,” in *ASM Handbook, Volume 11: Failure Analysis and Prevention*, (Materials Park: ASM International, 2021), 649–664.
  25. U. König and S. M. C. Verryn, “Heavy Mineral Sands Mining and Downstream Processing: Value of Mineralogical Monitoring Using XRD,” *Minerals* 11, no. 11 (2021): 1253. <https://doi.org/10.3390/min11111253>.
  26. Ch. V. G. K. Murty, J. Natarajan, and J. R. N. Rao, “Beneficiation of mineral sands: a practical outlook,” in *Mineral Processing: Beneficiation Operations and Process Optimization Through Modeling*, (Oxford: Elsevier/Academic Press, 2023), 167–220. <https://doi.org/10.1016/B978-0-12-823149-4.00005-3>.
  27. L. F. dos Santos Lara, G. F. C. Lima, L. Resende, and A. C. da Silva Bezerra, “Recent advances and perspectives of eco-efficient building materials from iron ore tailing: characterization, performance, and consumption,” *Journal of Cleaner Production* 505 (2025): 145488. <https://doi.org/10.1016/j.jclepro.2025.145488>.
  28. G. Asbjörnsson, L. M. Tavares, A. Mainza, and M. Yahyaee, “Different perspectives of dynamics in comminution processes,” *Minerals Engineering* 176 (2022): 107326. <https://doi.org/10.1016/j.mineng.2021.107326>.
  29. N. Chimwani, “Optimization of the Mechanical Comminution – The Crushing Stage,” in *Recovery of Values from Low-Grade and Complex Minerals*, 1st ed. (Hoboken: Wiley, 2024), 1–40.
  30. N. Rajendhran, K. Pondicherry, S. Huang, J. Vleugels, and P. De Baets, “Influence of abrasive characteristics on the wear micro-mechanisms of NbC and WC cermets during three-body abrasion,” *Wear* 530–531 (2023): 205007. <https://doi.org/10.1016/j.wear.2023.205007>.
  31. A. Jankovic, “Comminution and classification technologies of iron ore,” in *Iron Ore: Mineralogy, Processing and Environmental Sustainability*, 2nd ed., ed. L. Lu (Cambridge: Woodhead Publishing, 2022), 269–308. <https://doi.org/10.1016/B978-0-12-820226-5.00013-6>.
  32. D. Sterling, D. Schons, S. Breitung-Faes, and A. Kwade, “Effects of axial grinding media distribution on the disc wear behavior of a stirred media mill,” *Minerals Engineering* 185 (2022): 107702. <https://doi.org/10.1016/j.mineng.2022.107702>.
  33. P. J. Esteves, V. Seriacopi, M. C. S. de Macêdo, R. M. Souza, and C. Scandian, “Combined effect of abrasive particle size distribution and ball material on the wear coefficient in micro-scale abrasive wear tests,” *Wear* 476 (2021): 203639. <https://doi.org/10.1016/j.wear.2021.203639>.
  34. P. Seidel, D. Ebert, R. Schinke, et al., “Comparison of Elemental Analysis Techniques for the Characterization of Commercial Alloys,” *Metals* 11, no. 5 (2021): 736. <https://doi.org/10.3390/met11050736>.
  35. H. Usman, S. Fonna, S. Huzni, T. I. Ramadhan, and T. Octaviantana, “The Effect of Hardening on Mechanical Properties of Low Alloy Steel Grinding Media,” in *Proceedings of the 2nd International Conference on Experimental and Computational Mechanics in Engineering*, ed. AkhyarSingapore: Springer, 2021), 459–469. [https://doi.org/10.1007/978-981-16-0736-3\\_43](https://doi.org/10.1007/978-981-16-0736-3_43).
  36. B. C. Kandpal, D. K. Gupta, A. Kumar, et al., “Effect of heat treatment on properties and microstructure of steels,” *Materials Today: Proceedings* 44, part 1 (2021): 199–205. <https://doi.org/10.1016/j.matpr.2020.08.556>.
  37. L. Ling, L. Luo, and F. Liu, “Effects of grinding treatment on surface properties and deformation microstructure in alloy 304L,” *Surface and Coatings Technology* 408 (2021): 126850. <https://doi.org/10.1016/j.surfcoat.2021.126850>.
  38. B. Zhong, J. Dang, Q. An, and M. Chen, “Surface morphologies and microstructure of high-strength steel AISI 4820 with different heat treatment during grinding process,” *Journal of Manufacturing Processes* 96 (2023): 1–10. <https://doi.org/10.1016/j.jmapro.2023.04.045>.
  39. S. Y. Wang, X. Y. Hou, L. Wang, et al., “Effect of ball-milling process in combination with the addition of carbide microparticles on the microstructure and wear resistance of a Co–Cr–W alloy prepared by powder metallurgy method,” *Materials Research Express* 8, no. 6 (2021): 066506. <https://doi.org/10.1088/2053-1591/ac021f>.
  40. T. Liu, J. Sun, Z. Xiao, J. He, W. Shi, and C. Cui, “Effect of Multi-Element Microalloying on the Structure and Properties of High Chromium Cast Iron,” *Materials* 16, no. 9 (2023): 3292. <https://doi.org/10.3390/ma16093292>.
  41. S. Liu and L. Liang, “Research Progress on Alloying of High Chromium Cast Iron—Austenite Stabilizing Elements and Modifying Elements,” *Crystals* 15, no. 3 (2025): 210. <https://doi.org/10.3390/cryst15030210>.

42. A. Hatra, A. Salamah, and N. Aldaher, "Effect of Heat Treatment on the Microstructure, Impact Toughness and Hardness of High-Chromium White Cast Iron With Added Niobium and Manganese Minerals," *Al-Khwarizmi Engineering Journal* 21, no. 1 (2025): 73–88. <https://doi.org/10.22153/kej.2025.02.001>.
43. R. Jaramillo, D. F. Zambrano, P. Valenzuela, and C. A. Poblano, "Tribological Performance of High-Chromium Cast Irons: Effect of Chromium Content, Amount of Chromium Carbides ( $M_7C_3$ ) and Loading Conditions on Wear Resistance," *Tribology Letters* 73 (2025): 103. <https://doi.org/10.1007/s11249-025-02040-w>.
44. A. Fortini, A. Suman, A. Vulpio, M. Merlin, and M. Pinelli, "Microstructural and Erosive Wear Characteristics of a High Chromium Cast Iron," *Coatings* 11, no. 5 (2021): 490. <https://doi.org/10.3390/coatings11050490>.
45. E. Demirer, H. Pourasiabi, L. J. McInnes, R. Knibbe, and J. D. Gates, "Effects of Abrasive Rock Type on CVF-Dependent Performance Trends of White Cast Irons in the Inner Circumference Abrasion Test," *Tribology Transactions* 65, no. 3 (2022): 389–404. <https://doi.org/10.1080/10402004.2021.2020385>.
46. R. Jojith, M. Sam, and N. Radhika, "Recent advances in tribological behavior of functionally graded composites: A review," *Engineering Science and Technology, an International Journal* 25 (2022): 100999. <https://doi.org/10.1016/j.jestech.2021.05.003>.
47. Y. Huo, Y. Niu, Z. Sun, Y. Li, and J. Niu, "Surface/subsurface damage mechanisms and inhibition strategies in machining of hard and brittle materials: A systematic review," *Surfaces and Interfaces* 54 (2024): 105088. <https://doi.org/10.1016/j.surfin.2024.105088>.
48. A. Suman and A. Fortini, "Effects of Heat Treatment and Erosion Particle Size on Erosion Resistance of a Hypereutectic High-Chromium Cast Iron," *Coatings* 14, no. 1 (2024): 66. <https://doi.org/10.3390/coatings14010066>.
49. S. Gong, F. Wang, and K. Chen, "AlN and Nb(C,N) Composite Precipitation Behaviors and Their Effects on Austenite Grain Growth in SCr420H High-Temperature Carburized Gear Steel," *Steel Research International* 95, no. 7 (2024): 2400080. <https://doi.org/10.1002/srin.202400080>.
50. M. J. Huq, K. Shimizu, and K. Kusumoto, "Abrasive Wear Characteristics of High-Cr Multicomponent White Cast Irons at Elevated Temperatures," *Crystals* 15, no. 2 (2025): 113.
51. B. M. Rajcic, A. Maslarevic, G. M. Bakic, et al., "Erosion Wear Behavior of High Chromium Cast Irons," *Transactions of the Indian Institute of Metals* 76, no. 6 (2023): 1427–1437. <https://doi.org/10.1007/s12666-022-02860-7>.
52. X. Y. Yin and M. Chen, "Analysis of Grindability and Surface Integrity in Creep-Feed Grinding of High-Strength Steels," *Materials* 17, no. 8 (2024): 1784. <https://doi.org/10.3390/ma17081784>.
53. K. Kusumoto, K. Shimizu, R. H. Purba, and Y. Momma, "Effect of carbide refinement on high temperature erosive wear behavior of high chromium white cast iron with different titanium and carbon additions," *Materials Today Communications* 39 (2024): 109276. <https://doi.org/10.1016/j.mtcomm.2024.109276>.
54. M. Vakili, P. Koutník, J. Kohout, and Z. Gholami, "Analysis, Assessment, and Mitigation of Stress Corrosion Cracking in Austenitic Stainless Steels in the Oil and Gas Sector: A Review," *Surfaces* 7, no. 3 (2024): 589–642. <https://doi.org/10.3390/surfaces7030040>.
55. S. Rossi, F. Russo, A. M. Lemmi, M. Benedetti, and V. Fontanari, "Fatigue Corrosion Behavior of Friction Welded Dissimilar Joints in Different Testing Conditions," *Metals* 10, no. 8 (2020): 1018. <https://doi.org/10.3390/met10081018>.
56. G. Saha, K. Valtonen, A. Saastamoinen, P. Peura, and V. T. Kuokkala, "Impact-abrasive and abrasive wear behavior of low carbon steels with a range of hardness-toughness properties," *Wear* 450–451 (2020): 203263. <https://doi.org/10.1016/j.wear.2020.203263>.
57. Z. Wei, W. Wang, M. Liu, J. Tian, and G. Xu, "Comparison of wear performance of bainitic and martensitic structure with similar fracture toughness and hardness at different wear conditions," *Wear* 512–513 (2023): 204512. <https://doi.org/10.1016/j.wear.2022.204512>.
58. J. C. de Lacerda, R. L. P. Teixeira, W. D. dos Reis, P. H. S. Castro, L. S. de Oliveira, and R. A. G. de Lacerda, "Fracture analysis of a centrifugal ore slurry pump shaft: a study using fatigue tests, microstructural analysis and finite element simulation," *Multiscale and Multidisciplinary Modeling, Experiments and Design* 8 (2025): 83. <https://doi.org/10.1007/s41939-024-00675-1>.

### Supporting Information

The Universidade Federal de Itajubá (UNIFEI) is eligible under the CAPES-Wiley Transformative Agreement, allowing open access publication in hybrid Wiley journals without APCs, provided the corresponding author is affiliated with UNIFEI and complies with CAPES requirements, including ORCID ID and CC BY license.